Synthesis and Self-Assembly of Helical Polypeptide-Random Coil Amphiphilic Diblock Copolymer

SHIAO-WEI KUO,[1] HSIN-FANG LEE,[2] CHIH-FENG HUANG,[2] CHENG-JYNN HUANG,[2] FENG-CHIH CHANG[2]

[1]Department of Materials Science and Optoelectronic Engineering, Center for Nanoscience and Nanotechnology, National Sun Yat-Sen University, Kaohsiung, Taiwan

[2]Institute of Applied Chemistry, National Chiao Tung University, Hsin Chu, Taiwan

ABSTRACT: Three amphiphilic rod-coil diblock copolymers, poly(2-ethyl-2-oxazoline-*b*-γ-benzyl-L-glutamate) (PEOz-*b*-PBLG), incorporating the same-length PEOz block length and various lengths of their PBLG blocks, were synthesized through a combining of living cationic and *N*-carboxyanhydride (NCA) ring-opening polymerizations. In the bulk, these block copolymers display thermotropic liquid crystalline behavior. The self-assembled aggregates that formed from these diblock copolymers in aqueous solution exhibited morphologies that differed from those obtained in α-helicogenic solvents, that is, solvents in which the PBLG blocks adopt rigid α-helix conformations. In aqueous solution, the block copolymers self-assembled into spherical micelles and vesicular aggregates because of their amphiphilic structures. In helicogenic solvents (in this case, toluene and benzyl alcohol), the PEOz-*b*-PBLG copolymers exhibited rod-coil chain properties, which result in a diverse array of aggregate morphologies (spheres, vesicles, ribbons, and tube nanostructures) and thermoreversible gelation behavior. © 2008 Wiley Periodicals, Inc. J Polym Sci Part A: Polym Chem 46: 3108–3119, 2008

Keywords: block copolymer; hydrogen bonding; polypeptide; self-assembly; self-organization

INTRODUCTION

Many block copolymers self-assemble into ordered nanostructures in polymer melts[1–4] and/or in solution.[4–7] In melts, the phase behavior is largely controlled by the molecular architecture, that is, the degree of polymerization, the monomer composition, and the relative lengths of the blocks. In solutions, the interactions between the polymer and the solvent add an extra dimension, especially when the solvent is selective. A particular case is the self-assembly of solutions of amphiphilic block copolymers that consist of hydrophobic and hydrophilic blocks.[8] The self-assembly of amphiphilic block copolymers in block-selective solvents can result in a large range of nanoscale morphologies, including spheres, cylinders, vesicles, and layers.[8] The aggregation of rod-coil block copolymers is driven not only by the selectivity of the solvent but also by the tendency of the rigid segments to aggregate. The self-assembled structures formed from rod-coil block copolymers in selective solvents have been characterized experimentally[9–12] and predicted by theory[13–16] to differ distinctly from those of conventional coil-coil block copolymers.[6,8] The incorporation of helical chains as the rigid rod component of rod-coil copolymers is a particular valuable approach

toward creating novel supramolecular architectures.[11,17–21] Nevertheless, because of synthetic difficulties, only a few rod-coil block copolymers based on helical rods have been reported to date, including polyisocyanides,[11] polypeptides,[17–21] polyisocyanates,[22] and others.[23–24] In particular, block copolymers comprising of polypeptide segments provide a number of significant advantages when attempting to control both the function and supramolecular structure of bioinspired self-assembled systems.

Poly(γ-benzyl-L-glutamate) (PBLG) polymer is a synthetic polypeptide that assume a rigid α-helical conformation in solution and solid states.[25,26] PBLG forms aggregates in dilute solutions of some helicogenic poor solvents, such as benzene, toluene, benzyl alcohol, and mixed solvents of dioxane with fatty acids,[27–32] and exhibit thermoreversible gelation above certain critical concentrations.[33–41] The intrinsic rigidity of PBLG in the helicogenic solvents is due to stable intramolecular hydrogen bonding,[27] which results in such unique solution behavior as liquid crystalline ordering[42,43] and thermoreversible gelation. Solutions of PBLG are, therefore, useful models for research into the phase behavior of rod-like polymers. Manners and coworkers recently discovered that the thermoreversible gelation of the type PBLG-*block*-(random coil polymer) in a helicogenic solvent, toluene, occurs through a self-assembled nanoribbon mechanism,[44] which is distinct from that of the self-assembly of PBLG homopolymer.[41] PBLG is biodegradable and can form a hydrophobic core to function as a drug incorporation site.[45] Cho et al. reported the formation of polymer micelles composed of hydrophobic PBLG and hydrophilic poly(ethylene oxide) (PEO) or poly(*N*-isopropylacrylamide) (PNIPAAm) in aqueous environments.[46,47]

Poly(2-ethyl-2-oxazoline) (PEOz) is a water-soluble, nonionic, tertiary polyamide that exhibits low toxicity, high hydrophilicity,[48] and biocompatibility.[49,50] This unique combination of properties has led to its potential use in several applications.[51–53] Jeong and coworkers[54] reported the use of PEOz as the shell-forming polymer in poly(2-ethyl-2-oxazoline-*b*-DL-lactide), poly(2-ethyl-2-oxazoline-*b*-ε-caprolactone), and poly(2-ethyl-2-oxazoline-*b*-1,3-trimethylene carbonate) systems. The hydrophilic PEOz shells in these micelles undergo pH-sensitive hydrogen bonding with poly(methacrylic acid) (PMAA) and poly(acrylic acid) (PAA) in acidic aqueous media.

In this study, we synthesized a series of novel rod-coil amphiphilic diblock copolymers based on the coil hydrophilic PEOz polymer and the rod hydrophobic PBLG polymer by combining living cationic with *N*-carboxyanhydride (NCA) ring-opening polymerizations. The living cationic ring-opening polymerization of 2-ethyl-2-oxazoline is a facile synthetic route toward the preparation of hydroxyl-terminated PEOz. The terminal hydroxyl groups are converted through Mitsunobu reaction[55] into primary amino groups, which then initiate NCA ring-opening polymerization of γ-benzyl-L-glutamate NCA to form the amphiphilic diblock copolymer poly(2-ethyl-2-oxazoline-*b*-γ-benzyl-L-glutamate) (PEOz-*b*-PBLG). We investigate the aggregation behaviors of these diblock copolymers in the bulk, in solvents that are α-helicogenic for the PBLG blocks. In the bulk, these block copolymers exhibited thermotropic liquid crystalline behavior; in aqueous solution, they self-assembled into spherical micelles and vesicular aggregates because of their amphiphilic nature; in solvent that are helicogenic for PBLG blocks, (in this case, toluene and benzyl alcohol), the PEOz-*b*-PBLG copolymers exhibited rod-coil chain properties, which led to a diverse range of aggregate morphologies (spheres, vesicles, ribbons, and tube nanostructures) and thermoreversible gelation behavior.

EXPERIMENTAL

Materials

2-Ethyl-2-oxazoline (Aldrich) was dried and vacuum-distilled over calcium hydride. Methyl *p*-toluenesulfonate (Aldrich) was purified by vacuum distillation. Acetonitrile was distilled over calcium hydride. Triphenylphosphine (TPP; Acros), phthalimide (PI; Fluka), diethyl azodicarboxylate (DEAD; 40 wt % in toluene; Aldrich), tetrahydrofuran (THF; anhydrous, inhibitor-free; Aldrich), *N,N*-dimethylformamide (DMF; anhydrous; Aldrich), and hydrazine monohydrate were used as received. γ-Benzyl-L-glutamate *N*-carboxyanhydride (Bn-Glu NCA) was prepared according to a literature procedure[56] and stored at −30 °C. Water was purified through distillation, deionization, and osmosis. Other solvents, including diethyl ether, toluene, and benzyl alcohol, were used without further purification.

Synthesis of Hydroxyl-Terminated Poly(2-ethyl-2-oxazoline) (Me-PEOz-OH)

2-Ethyl-2-oxazoline (30.0 g, 303 mmol) was added via a syringe to a solution of methyl p-toluenesulfonate (2.25 g, 12 mmol) in acetonitrile (100 mL). The polymerization mixture was stirred under reflux for 240 h under an argon atmosphere. The mixture was cooled to room temperature and treated with methanolic KOH (0.1 N) to quench the poly(2-ethyl-2-oxazoline) oxazolinium living end group and to introduce the hydroxyl group at the end of the PEOz chain. The product, "Me-PEOz-OH," was isolated following a literature procedure.[57]

Mitsunobu Conversion of Terminal Hydroxyl Groups into Terminal Primary Amino Groups (Me-PEOz-NH₂)

Me-PEOz-OH (M_n = 2100) (4.2 g, 2 mmol) was added to a stirred solution of TPP (15.75 g, 60 mmol) and PI (9 g, 60 mmol) in THF (50 mL). DEAD (d = 0.95 g/mL; 10.5 g, 12 mL, 60 mmol) was then added dropwise to the mixture under an argon atmosphere. After being maintained at room temperature for 24 h, the mixture was dialyzed first against ethanol and then against distilled water using a Spectrapor dialysis membrane having an M_r molecular weight cutoff of 1000. The solution was lyophilized for 2 days to yield the phthalimide-activated polymer "Me-PEOz-PI." This material (3 g, 0.6 mmol) was then dissolved in ethanol (250 mL) and treated with hydrazine monohydrate (250 mL). The mixture was maintained at room temperature for 24 h. After the ethanol had been evaporated, an aqueous sodium hydroxide was added up to pH 9–10. The polymer was extracted with methylene chloride, and then purified through dialysis against ethanol and distilled water using a Spectrapor dialysis membrane with a M_r cutoff 1000. Lyophilization of the dialyzed solution gave the amino-terminated polymer "Me-PEOz-NH₂."

Synthesis of PEOz-*b*-PBLG Diblock Copolymers

A Schlenk flask fitted with a stirrer bar and drying tube was charged with the appropriate amount of Bn-Glu NCA in dry DMF (0.1 g/mL). The required amount of primary amino-terminated PEOz was added, and then the reaction mixture was stirred at room temperature. After

5 days, the block copolymer was precipitated in diethyl ether, filtered, and vacuum-dried. The resultant product was extracted with methanol in a Soxhlet extractor for 3 days to remove the soluble nonfunctionalized PEOz macroinitiator; finally, dried at 40 °C *in vacuo*.

Preparation of Micelle Solutions

Experiments in Aqueous Solution

Micelles of PEOz-*b*-PBLG block copolymers were prepared using a method based on dialysis.[58] The block copolymer (10 mg) was dissolved in DMF (2 mL), and then stirred overnight at room temperature. To form micelles, the solution was dialyzed against distilled water for 40 h using a Spectrapor dialysis membrane (molecular weight cutoff: 3500).

Experiments in Toluene and Benzyl Alcohol

PEOz-*b*-PBLG/toluene or PEOz-*b*-PBLG/benzyl alcohol solutions were prepared by adding filtered toluene or filtered benzyl alcohol to the block copolymer sample in a sealed vial. The solution (without further filtration) was heated until the mixture became homogeneous, and then annealed for 2 h before being cooled to room temperature to allow equilibrium to be reached. Solutions were identified by the weight fraction of polymer, w.

During the cooling process, some of the solution samples exhibited thermally reversible gelation behavior. We defined such a state as a gel in which no flow occurred in the sample solution. The lowest concentration for such gelation was designated as C_{gel}. The values of T_{gel} were measured using the procedure reported by Hirst and coworkers[59] All values of C_{gel} and T_{gel} were measured three times.

Characterizations

Both the molecular weight and molecular weight distribution were determined through gel permeation chromatography (GPC) using a Waters 510 HPLC equipped with a 410 differential refractometer, a refractive index (RI) detector, and three Ultrastyragel columns (100, 500, and 103 Å) connected in series in order of increasing pore sizes. DMF was used as an eluent at a flow rate of 0.6 mL/min. ¹H NMR spectra were recorded at room temperature on a Bruker AM

500 (500 MHz) spectrometer, using the residual proton resonance of the deuterated solvent as the internal standard. Thermal analysis through differential scanning calorimetry (DSC) was performed using a DuPont 910 DSC-9000 controller at a scan rate of 10 °C/min over a temperature range from −100 to 180 °C under a nitrogen atmosphere. Transmission electron microscopy (TEM) was performed on a Hitachi H-7500 electron microscope operated at 100 kV. For the solution sample, a drop of the sample solution was placed onto a 200-mesh copper grid coated with carbon. About 2 min after deposition, the grid was tapped with a filter paper to remove the surface solution, followed by air-drying. For gel samples, a carbon-coated copper grid was gently placed on the fraction of gel. The copper grid was removed after 30 s and air-dried for 1 h. To enhance the contrast, the sample specimen was stained with the vapor of an aqueous solution of RuO_4. The sample was air-dried prior to measurement. X-ray diffraction (XRD) measurements were performed using the wiggler beamline BL17A1 of the National Synchrotron Radiation Research Center (NSRRC), Taiwan. A triangular bent Si(111) single crystal was employed to obtain a monochromatic beam having a wavelength (λ) of 1.3344 Å. The XRD patterns were collected using a curved imaging plate (IP; Fuji BAS III, area = 20 × 40 cm^2) having a radius equivalent to the sample-to-detector distance of 280 mm. With the 100-μm pixel resolution of the IP and a typical exposure time of 15 min, the XRD patterns were measured cover a range of values of q from 0.01 to 2.2 Å^{-1}, where the X-ray vector transfer $q = 4\pi$ $\sin(\theta)/\lambda$ is defined by the scattering angle 2θ and λ. The two-dimensional X-ray diffraction patterns observed for the sample (typical diameter 10 mm; thickness 1 mm) were circularly averaged to provide a one-dimensional diffraction profile $I(q)$, with the value q value calibrated using standard samples of Ag-Behenate and Si powder (NBS 640b).

RESULTS AND DISCUSSION

Syntheses and Properties of PEOz-*b*-PBLG Diblock Copolymers

Scheme 1 outlines our synthetic the strategy toward the PEOz-*b*-PBLG diblock copolymer. Cationic ring-opening polymerization of 2-ethyl-2-
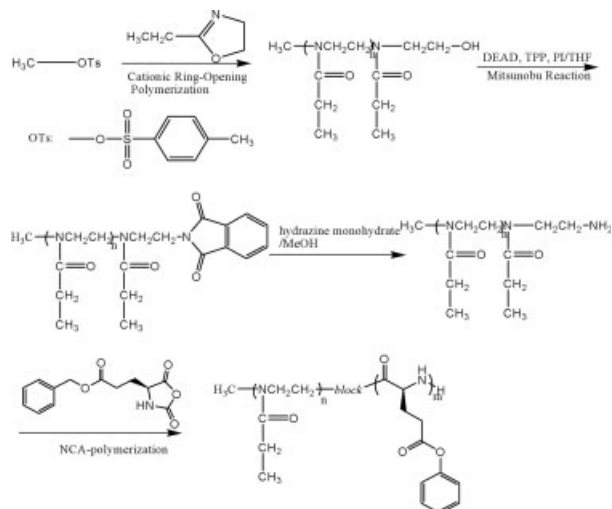
Scheme 1. Synthesis of PEOz-*b*-PBLG block copolymers.

oxazoline (initiated by methyl *p*-toluenesulfonate), produced the poly(2-ethyl-2-oxazoline) bearing a hydroxyl group at one end (Me-PEOz-OH). Next, the terminal hydroxyl unit of Me-PEOz-OH was converted into a primary amino group, which was able to further conjugate with the polypeptide through NCA-polymerization. This transformation was performed in good yield through a two step Mitsunobu reaction: (1) the conversion of the terminal hydroxyl group into a phthalimido unit and (2) subsequent treatment with hydrazine to generate the free amine. The nature of the end-group was transformation was characterized using ^{1}H NMR spectroscopic analysis (Fig. 1). In the ^{1}H NMR spectrum of the hydroxyl-terminated polymer [Me-PEOz-OH; Fig. 1(a)], the signal at 3.59 ppm can be ascribed to the methine protons of PEOz that are attached to the hydroxyl end group. Conversion of the end group into a phthalimide unit (Me-PEOz-PI) was confirmed by the appearance of signals at 3.78 and 4.19 ppm (methine protons attached to phthalimide) and the disappearance of the signal at 3.59 ppm, as indicated in Figure 1(b). After treatment with hydrazine, Figure 1(c) reveals the loss of the ω-terminal phthalimide group through the disappearance of the signals at 3.78 and 4.19 ppm, and the appearance of a signal at 2.73 ppm representing the primary amino-terminated polymer (Me-PEOz-NH$_2$). Next, we used Me-PEOz-NH$_2$ to initiate the polymerization of γ-benzyl-L-glutamate *N*-carboxyanhydride (Bn-Glu NCA), which was conducted in DMF solution at room temperature
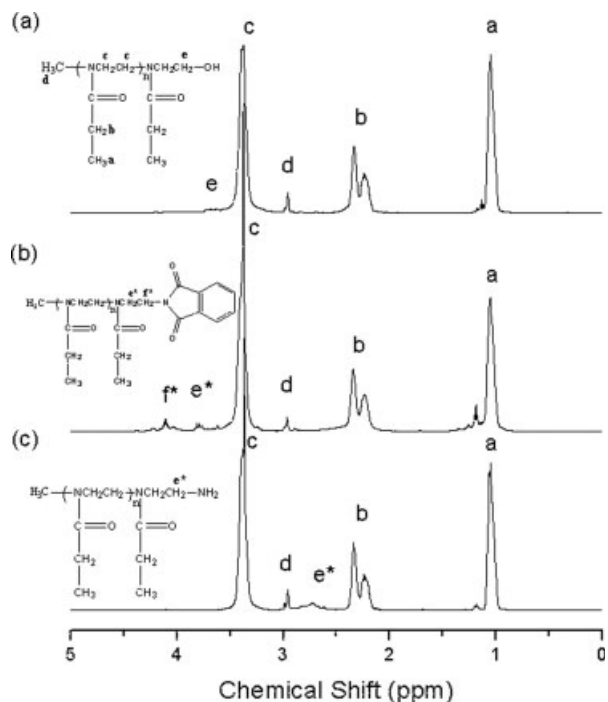
Figure 1. ^{1}H NMR spectra of (a) Me-PEOz-OH, (b) Me-PEOz-PI, and (c) Me-PEOz-NH$_2$ in CDCl$_3$.

under the exclusion of moisture, over a period of 5 days. The length of the γ-benzyl-L-glutamate segment was controlled by adjusting the molar ratio of the Bn-Glu NCA and the primary amino end-functionalized PEOz initiator. All of the diblock copolymers described herein were prepared using primary amino-terminated PEOz having a number-average degree of polymerization of 21 (Me-PEOz$_{21}$-NH$_2$). After precipitation and drying, these PEOz-b-PBLG copolymers were characterized using ^{1}H NMR spectroscopy [Fig. 2(a)] and GPC [Fig. 2(b)]; Table 1 summarizes the results. The desired block copolymers were obtained in good yields.

The bulk properties of these PEOz-b-PBLG copolymers were characterized through DSC and XRD measurements. The DSC thermograms in Figure 3 indicate that the PEOz polymer having an M_n of 2100 possesses a glass transition temperature at $\sim$ 50 °C, and that the PEOz-b-PBLG copolymer exhibits a nematic-like liquid crystal (LC) phase transition at $\sim$ 100 °C during the first heating run.[22,60] During the second heating run, we observed only one glass transition temperature (at $\sim$ 45 °C) for the copolymer. Figure 4 presents the one-dimensional XRD patterns for PEOz$_{21}$-b-PBLG$_{26}$, PEOz$_{21}$-b-PBLG$_{56}$, and PEOz$_{21}$-b-PBLG$_{68}$ obtained at 120 °C, a

temperature at which the PEOz and PBLG blocks should be in their molten and liquid-crystalline states, respectively. We observe an amorphous halo at a high value of $q = 1.4$ Å^{-1}, with the halo maximum presenting a d spacing of 0.45 nm, indicating the molten state of the PEOz at 120 °C. In the medium-q region, we detected a set of Bragg peaks at $q = 0.45$, 0.78, and 0.90 Å^{-1} having a ratio of 1:3$^{1/2}$:2, corresponding to a columnar hexagonal organization of the peptide α-helices with a lattice parameter of $\sim$ 14 Å.[22,60] This set of characteristic peaks was present in the XRD patterns of all three of the copolymers. In addition, in Figure 4(a) we observe one additional peak at a lower q value (0.32 Å^{-1}) for PEOz$_{21}$-b-PBLG$_{26}$; this signal corresponds to a change in the peptide chain organization to a lamellar state having a β-sheet secondary structure, induced through destabilization of the α-helical secondary structure upon decreasing the length of the peptide chain.[22,60] Furthermore, we detected no peaks for any of
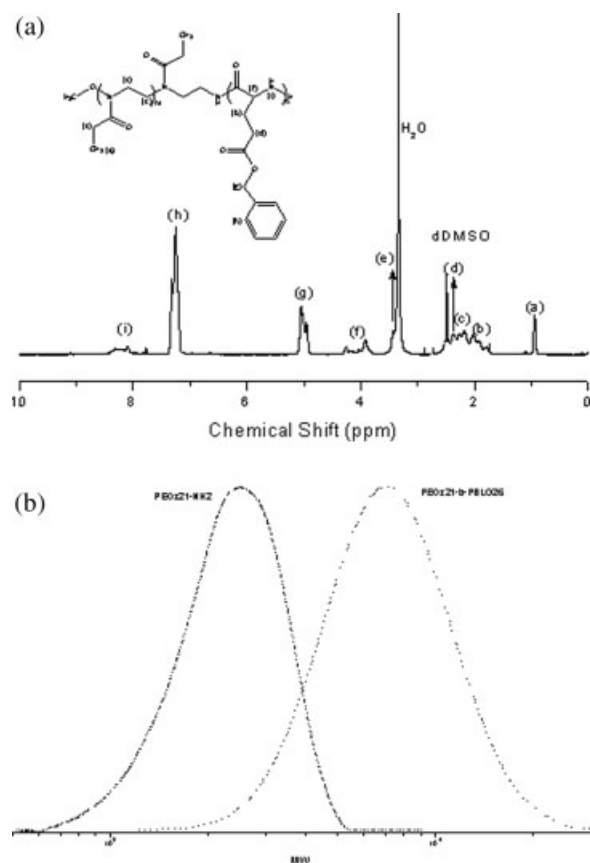
Figure 2. (a) ^{1}H NMR spectra of PEOz$_{21}$-b-PBLG$_{56}$ in d_6-DMSO and (b) GPC trace of PEOz$_{21}$-b-PBLG$_{26}$.

Table 1. Molecular Weight Characteristics of Block Copolymers

Sample	Yield (%)[a]	M_n[b]	Block Ratio[b] (PEOZ/PBLG)	M_w/M_n[c]
PEOz$_{21}$-NH$_2$	93	2100	–	1.08
PEOz$_{21}$-*b*-PBLG$_{26}$	58	7790	1:1.2	1.18
PEOz$_{21}$-*b*-PBLG$_{56}$	63	14,300	1:2.6	1.23
PEOz$_{21}$-*b*-PBLG$_{68}$	65	17,000	1:3.2	1.30

[a] Isolated yield, after precipitation and drying.
[b] Number-average molecular weight of the peptide segment, determined from the ^{1}H NMR spectrum (DMSO-d_6).
[c] From GPC, GPC experiments performed using DMF.

these three block copolymers from small-angle X-ray scattering (SAXS) experiments in the low q region, indicating that no long-range ordering is present in these block copolymers in the bulk state. We speculate that the PEOz and PBLG blocks are partially miscible and, thus, the copolymers lack long-range-ordered microphase separated structures in the bulk state. In addition, the value of T_g of the copolymers were lower than that (50 °C) of the PEOz homopolymer (Fig. 3).

Aggregates of PEOz-*b*-PBLG in Aqueous Solution

Because of the amphiphilic nature of the diblock copolymers, we expected that the PEOz and PBLG blocks would phase-separate in aqueous solution. We used ^{1}H NMR spectroscopy to monitor the phase separation behavior of these block copolymers in an aqueous phase. As indicated in the ^{1}H NMR spectrum of PEOz$_{21}$-*b*-PBLG$_{56}$ in d_6-DMSO (Fig. 2), in which micelle formation was not expected, the characteristic peaks of the protons of the benzyl groups and the methylene
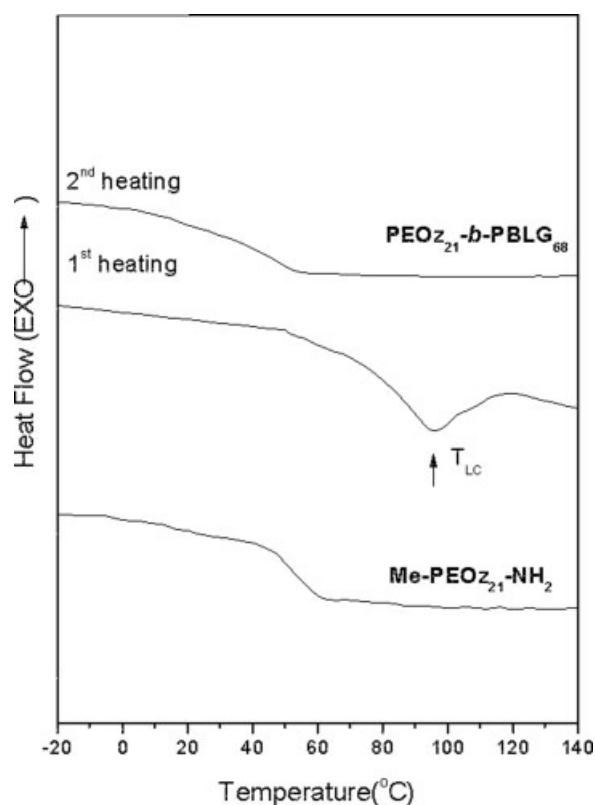
Figure 3. DSC thermograms of (a) Me-PEOz$_{21}$-NH$_2$ and (b) PEOz$_{21}$-*b*-PBLG$_{68}$.
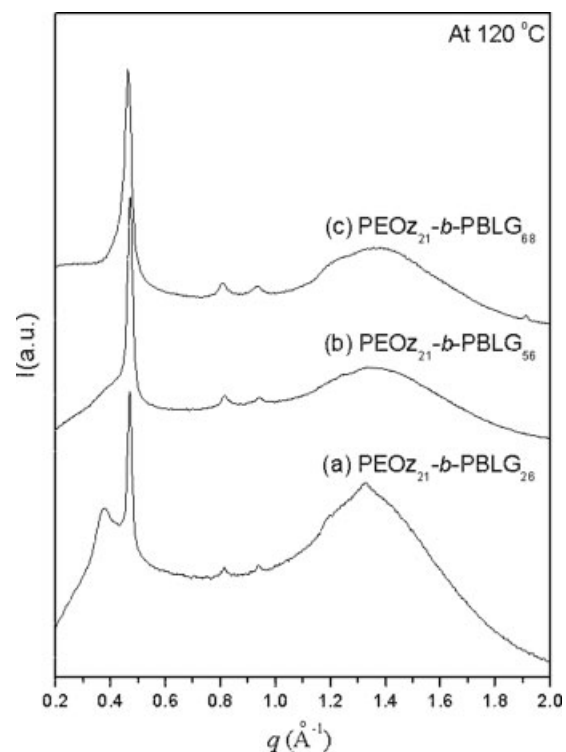
Figure 4. XRD patterns obtained at 120 °C for (a) PEOz$_{21}$-*b*-PBLG$_{26}$, (b) PEOz$_{21}$-*b*-PBLG$_{56}$, and (c) PEOz$_{21}$-*b*-PBLG$_{68}$ in their bulk states.
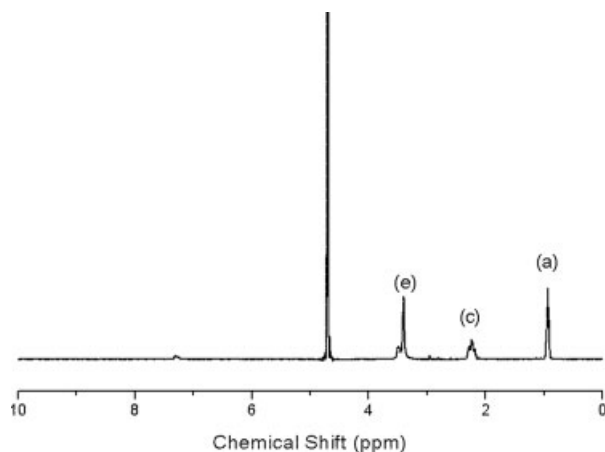
**Figure 5.** ^{1}H NMR spectrum of PEOz$_{21}$-*b*-PBLG$_{56}$ in D$_2$O.

protons adjacent to the benzyl groups of the PBLG segment appear at 7.2 and 5.0 ppm, respectively. In contrast, these peaks disappeared when the copolymer was dissolved in D$_2$O (Fig. 5). This result indicates the restricted motion of these protons within a micellar core of the rigid hydrophobic PBLG units surrounded by the hydrophilic PEOz moieties in the PEOz-*b*-PBLG polymeric micelles. We used TEM to examine the morphologies of the PEOz$_{21}$-*b*-PBLG$_{26}$, PEOz$_{21}$-*b*-PBLG$_{56}$, and PEOz$_{21}$-*b*-PBLG$_{68}$ copolymers in aqueous solution. Figure 6 presents images of the spherical micelles formed from the PEOz$_{21}$-*b*-PBLG$_{26}$ and PEOz$_{21}$-*b*-PBLG$_{56}$ copolymers and the near vesicle-like structure obtained from the PEOz$_{21}$-*b*-PBLG$_{68}$ copolymer. These results demonstrate that PEOz-*b*-PBLG copolymers may be useful for drug delivery applications in which site-specific delivery is mediated by synthetic polymer-protein interactions.

Aggregates of PEOz-*b*-PBLG in Helicogenic Solvents for PBLG Blocks

In poorly helicogenic solvents, PBLG adopts a rigid α-helical conformation; thus, we expected that PEOz-*b*-PBLG would exhibit coil-rod chain properties, leading to interesting aggregation behavior different from that of coil-coil block copolymers. Theoretical studies into the possible equilibrium structures of micelles of rod-coil block copolymers in solvents selective solvent for the coil block have been described.[13,15] The differences between the structures of coil-coil and rod-coil aggregates in selective solvents are traceable to their core structures: (i) The configuration of a rigid, rod-like block is, by definition, unique. No configurational change is thus expected upon aggregation. As a result, there is no free-energy penalty due to the deformation of the core block in rod-coil aggregates. Their growth is dominated by the penalty associated with the intercoronal chain interaction and the core-coronal interfacial energy; this feature differs from that of their coil-coil counterparts, where chain stretching of the core is an important factor. (ii) Aggregated rods are expected to favor ordered packing with their long axes aligned. The geometries of rod-coil assemblies are, accordingly, different. For our present system, we used TEM and X-ray diffraction measurements to investigate the aggregates formed from PEOz-*b*-PBLG rod-coil diblock copolymers (having three different block ratios) in two kinds of solvents that are poorly helicogenic for the PBLG block (toluene and in benzyl alcohol). TEM samples were prepared through the dripping of the aggregated solutions onto copper grids; the aggregates were stained with an aqueous solution of RuO$_4$.
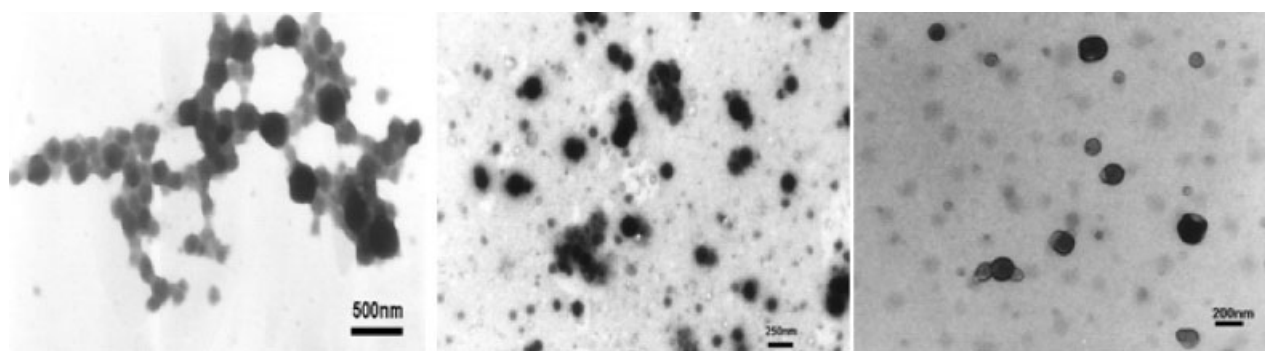
Figure 6. TEM images of the aggregates formed from (a) PEOz$_{21}$-*b*-PBLG$_{26}$, (b) PEOz$_{21}$-*b*-PBLG$_{56}$, and (c) PEOz$_{21}$-*b*-PBLG$_{68}$ at polymer concentrations of 0.5 wt % in aqueous solutions. Samples were observed after RuO$_4$ staining.
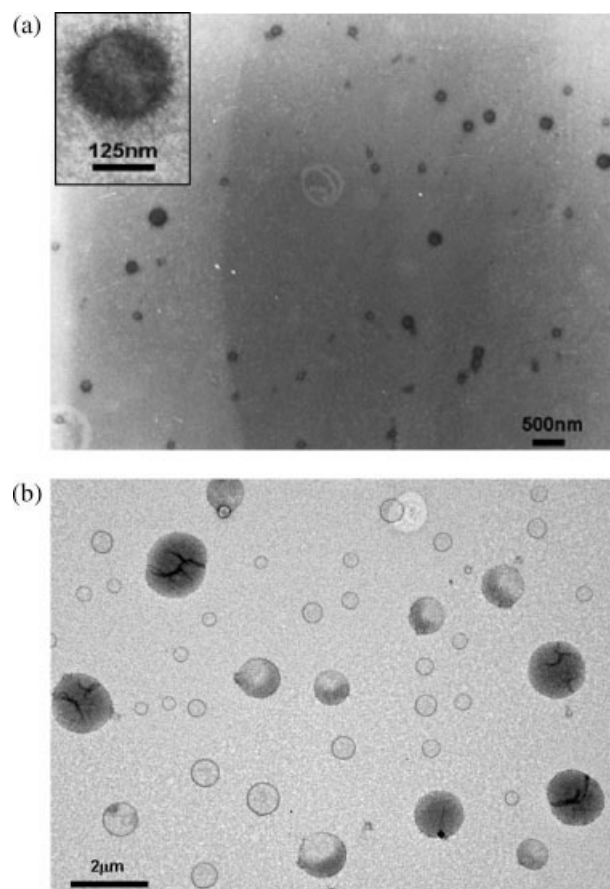
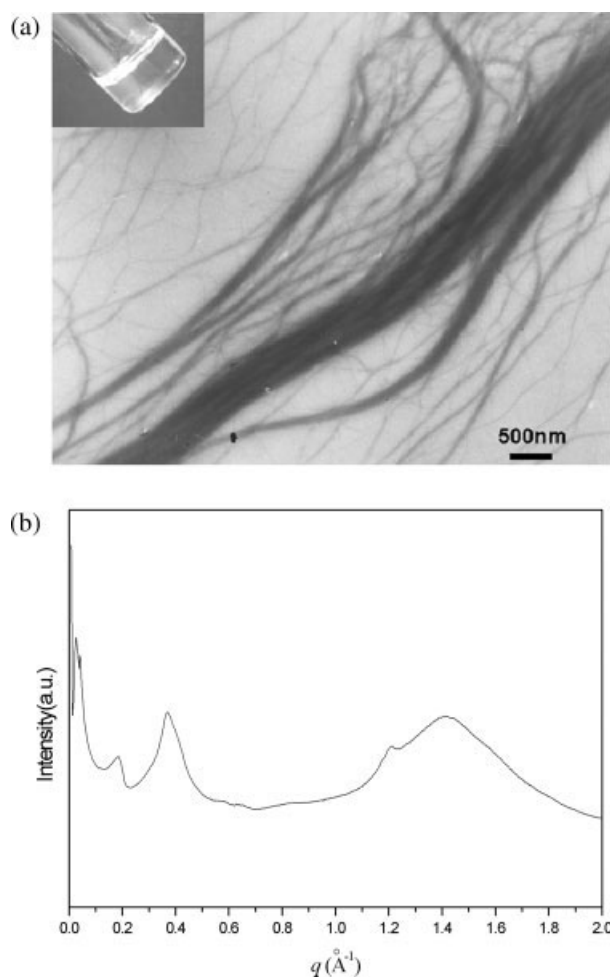**Figure 7.** TEM images of aggregates formed from (a) $PEOz_{21}$-*b*-$PBLG_{26}$ and (b) $PEOz_{21}$-*b*-$PBLG_{56}$ at a polymer concentration of 0.5 wt % in toluene. Samples were observed after RuO_4 staining.

Toluene is a good solvent for PEOz-*b*-PBLG at high temperature (>90 °C); at room temperature, however, it is a good solvent for the coil PEOz but a poor solvent for the rod PBLG. Therefore, the block copolymer self-assembles when its toluene solution is cooled from elevated temperature to room temperature. Figures 7 and 8(a) display the various morphologies formed from 0.5 wt % toluene solutions of PEOz-*b*-PBLG copolymers having different ratios of their insoluble/soluble block lengths. Bilayer-type vesicle structures [Figs. 7(a,b)] were formed by the $PEOz_{21}$-*b*-$PBLG_{26}$ and $PEOz_{21}$-*b*-$PBLG_{56}$ copolymers, respectively. Rod-coil diblock copolymers have a strong tendency to form bilayer structures in selective solvents because of the intrinsic orientational order of the rigid-rod blocks.[61] Here, the rod-like α-helical PBLG chains tend to pack in the unfavorable toluene solvent to minimize the interfacial energy between the rod block and the solvent;

they form, according to the "hockey puck" model, finite-sized cylindrical discs [Scheme 2(a)] covered by coil segments.[61] Vesicles are formed when the bilayer disc-like aggregates are large and the energy loss due to surface tension effects is so great that it results in hull closure [Scheme 2(b)]. Bending of the bilayer disc-like aggregates into closed vesicles requires a bending energy. The vesicle size (R_v) can be defined using the expression $R_v = 2\kappa/\gamma$,[61] where κ is the bending modulus and γ is the surface tension of the rim of the bilayer disc. Increasing order inherently leads to an increase of the bending modulus of the bilayer. Comparing Figures 7(a,b), we observe that the vesicle size of $PEOz_{21}$-*b*-$PBLG_{56}$ was substantially larger than that of $PEOz_{21}$-*b*-$PBLG_{26}$. We attribute this size

Figure 8. (a) TEM images of the aggregates (RuO_4 stained) formed from $PEOz_{21}$-*b*-$PBLG_{68}$ at a polymer concentration of 0.5 wt % in toluene and (b) XRD patterns of a dried film of the assemblies formed from $PEOz_{21}$-*b*-$PBLG_{68}$ in toluene.
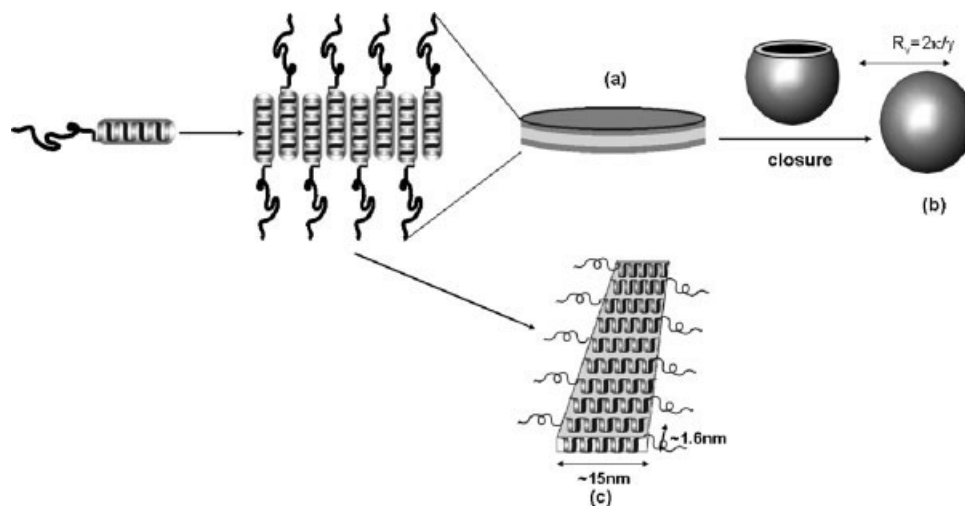
Scheme 2. Schematic representations of the (a) formation of bilayers and (b) their closure to vesicles for the PEOz$_{21}$-*b*-PBLG$_{26}$ and PEOz$_{21}$-*b*-PBLG$_{56}$ copolymers in toluene. (c) Nanoribbon structure formed in the network structure of the toluene gel of PEOz$_{21}$-*b*-PBLG$_{68}$.

difference to the increase of in the bending modulus (κ) of the bilayer that occurred upon increasing the PBLG block length. Figure 8(a) indicates that, with its long α-helical rigid PBLG block and a relatively lower PEOz content, the PEOz$_{21}$-*b*-PBLG$_{68}$ copolymer formed a fibrous structure. In addition, the toluene solution of PEOz$_{21}$-*b*-PBLG$_{68}$ underwent thermoreversible gelation with the values of T_{gel} and C_{gel} of 46 °C and 0.4 wt %, respectively. Manners and coworkers noted that the thermoreversible gelation of diblock copolymers of the type PBLG-*block*-(random coil polymer) in toluene (a helicogenic solvent) occurred through a self-assembled nanoribbon mechanism.[44] Thus, we suggest that the fibrous morphology is, in fact, a ribbon-like nanostructure exhibiting, as its long axis, PBLG helices oriented in an antiparallel manner on the plane of the ribbon [see Scheme 2(c)] to minimize the degree of steric repulsion between PEOz chains. The dissimilar morphologies of the PEOz$_{21}$-*b*-PBLG$_{68}$ nanoribbons and the PEOz$_{21}$-*b*-PBLG$_{26}$ and PEOz$_{21}$-*b*-PBLG$_{56}$ vesicles are due to the presence of the longer PBLG block in the PEOz$_{21}$-*b*-PBLG$_{68}$ copolymer; because the length of the PBLG rod in this case was significantly longer than that of the coil block, the degree of corona repulsion between the PEOz coil chains was relatively weak and, as a result, the rods favored ordered packing with their long axes aligned. We performed X-ray diffraction measurements on the dried toluene gel of

PEOz$_{21}$-*b*-PBLG$_{68}$ because this gel exhibited strong birefringence, indicating the presence of regular structure, when examined under a polarized optical microscope. In Figure 8(b), the diffraction peak observed at $q = 0.4$ Å^{-1} (1.6 nm) indicates the distance between the PBLG helices; the peak at $q = 0.04$ Å^{-1} ($\sim$ 15 nm) is consistent with the width of the individual ribbons as measured using TEM. The additional diffraction peak at $q = 0.2$ Å^{-1} (3.1 nm) probably arose from the arrangement of the PEOz coil.

As is the case in toluene, these PEOz-*b*-PBLG diblock copolymers are also soluble in benzyl alcohol at higher temperatures, although it is a poor solvent for PBLG rods at lower temperatures. Benzyl alcohol is, however, a better solvent than toluene for the PEOz block. Thus, we expected a more expanded corona for the PEOz coil and greater stretching of the PEOz chains in benzyl alcohol than were observed in toluene. From this perspective, we also expected stronger repulsive interactions among the intercoronal chains for the PEOz block in benzyl alcohol than in toluene. Figures 9 and 10(a) present images of the aggregates formed from PEOz$_{21}$-*b*-PBLG$_{26}$, PEOz$_{21}$-*b*-PBLG$_{56,}$ and PEOz$_{21}$-*b*-PBLG$_{68}$ copolymers, each at a concentration of 0.5 wt % in benzyl alcohol. With its relatively longer swollen hydrophilic PEOz block in benzyl alcohol, the PEOz$_{21}$-*b*-PBLG$_{26}$ copolymer formed spherical micelles [Fig. 9(a)] having a PBLG core and a PEOz shell.
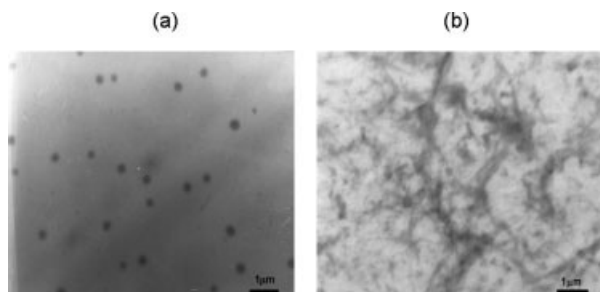
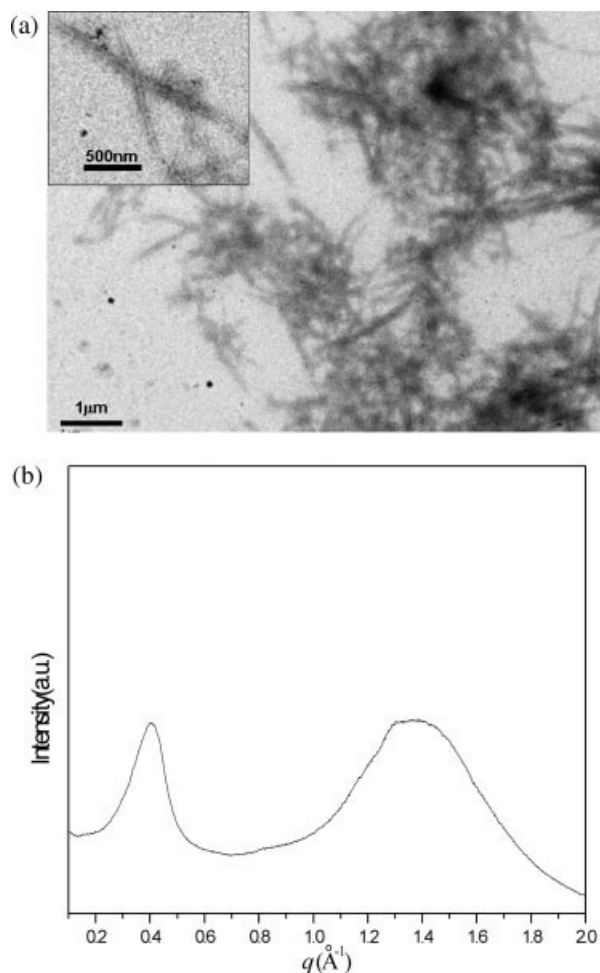**Figure 9.** TEM images of the aggregates formed from (a) $PEOz_{21}$-*b*-$PBLG_{26}$ and (b) $PEOz_{21}$-*b*-$PBLG_{56}$ at a polymer concentration of 0.5 wt % in benzyl alcohol. Samples were observed after RuO_4 staining.

When the length of the PEOz unit is relatively long, the repulsive interactions among the inter-coronal chains outweigh the attractive interfacial interactions and dominate the equilibrium structure. Therefore, the block copolymer favors the formation of star-like spherical micelles possessing extended PEOz coronas. When the relative length of the PBLG block is increased (i.e., for $PEOz_{21}$-*b*-$PBLG_{56}$), the coronal repulsion becomes relatively weak and irregular structures incorporating some cylinders and small spheres are formed [Fig. 9(b)]. The formation of cylinders, rather than spherical micelles, is probably due to the smaller surface area per PEOz coil chain and, thus, a lower total interfacial energy. For the $PEOz_{21}$-*b*-$PBLG_{68}$ copolymer, with its long α-helical rigid PBLG block and a low PEOz content, the tube-like structure is observed for copolymer as presented in Figure 10(a). We infer that this tube-like structure grew, at the expense of the spheres, through fusion or coalescence. Evidence for this type of growth mechanism was reported by Winnik and coworkers for the self-assembly of crystalline-coil poly(ferrocenylsilane)-*block*-poly(siloxane) in *n*-hexane and *n*-decane.[62] The solubility of PEOz in benzyl alcohol increases upon increasing the temperature. When we heated the solution until the mixture became homogeneous, the resulting PEOz corona chains became more swollen. Steric repulsion among the corona chains promotes curvature at the core-corona interface to increase the volume accessible to each corona chain; when the solution is cooled from high temperature to room temperature, the PEOz chains contract and this steric repulsion is diminished. Thus, the cooling of a sample favors a decrease in the curvature of its interface. Under normal circumstances, this deswelling provides a driving force for the diameter of the core to

increase. We speculate that the dense core of the cylindrical structure having long PBLG rods may not be able to accommodate a decrease in curvature, which would require a rearrangement of the insoluble rod PBLG block to fill the volume of the core. Rearrangement to a hollow structure with PEOz chains protruding from both the interior and exterior surfaces (Scheme 3) may provide an optimum balance. We also performed X-ray diffraction measurements using the film of $PEOz_{21}$-*b*-$PBLG_{68}$ cast from the benzyl alcohol solution. In Figure 10(b), the diffraction peak at $q = 0.4$ $Å^{-1}$ (1.6 nm) indicates the distance between the PBLG helices.

In summary, in this study, we have demonstrated that regular α-helical structures can be

Figure 10. (a) TEM images of the aggregates (RuO_4 stained) formed from $PEOz_{21}$-*b*-$PBLG_{68}$ at a polymer concentration of 0.5 wt % in benzyl alcohol and (b) XRD patterns of a dried film of the assemblies formed from $PEOz_{21}$-*b*-$PBLG_{68}$ in benzyl alcohol.
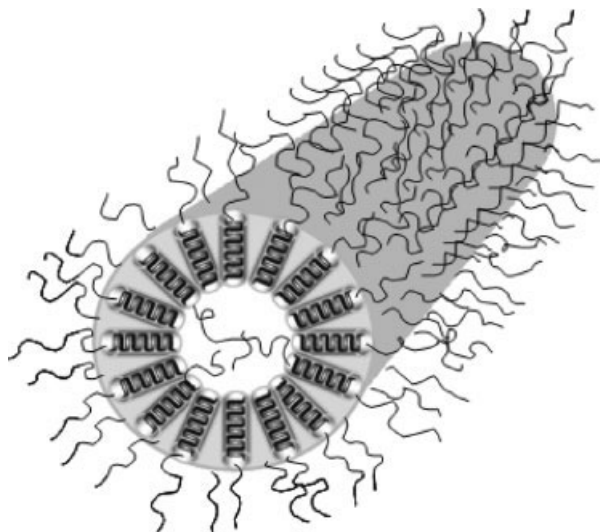
Scheme 3. Schematic representation of a tube nanostructure formed by PEOz$_{21}$-b-PBLG$_{68}$ in benzyl alcohol. The PEOz chains are depicted as coils, the PBLG units as dark helical rods.

produced on the nanoscale by exploiting the specific assembling properties of rod-coil PBLG-b-PEOz block copolymers. Fine-tuning of the morphologies and lateral dimensions of these nanostructures is possible through synthesis control of the block lengths and judicious choice of the solvent.

CONCLUSIONS

In this article, we describe the multistep synthesis of novel amphiphilic rod-coil PEOz-b-PBLG copolymers through cationic and N-carboxyanhydride ring-opening polymerizations. We prepared three PEOz-b-PBLG copolymers that had the same PEOz length but different lengths of their PBLG units. In the bulk, these block copolymers exhibit thermotropic liquid crystalline behavior. In aqueous solution, they self-assemble into spherical micelles or vesicular-like aggregates because of their amphiphilic nature. In helicogenic solvents for PBLG blocks, toluene and benzyl alcohol, the PEOz-b-PBLG copolymers exhibits rod-coil chain properties that result in diverse aggregate morphologies (spheres, vesicles, ribbons, and tube nanostructures) and thermoreversible gelation behavior. We employed TEM and XRD measurements to identify the morphologies of aggregates that self-assembled from these diblock copolymers in

solution. Synthetic control over the block lengths and the judicious choice of solvent allow fine-tuning of the morphologies and lateral dimensions of these nanostructures.

REFERENCES AND NOTES

1. Muthukumar, M.; Ober, C. K.; Thomas, E. L. Science 1997, 277, 1225–1232.
2. Stupp, S. I.; Braun, P. V. Science 1997, 277, 1242–1248.
3. Ryan, A. J.; Hamley, I. W. In The Physics of Glassy Polymers; Haward, R. N.; Yang, R. J., Eds.; Chapman and Hall: London, 1997.
4. Hamley, I. W. The Physics of Block Copolymers; Oxford University Press: Oxford, England, 1998.
5. Booth, C.; Price, C. Comprehensive Polymer Science; Pergamon Press: Oxford, England, 1989.
6. Tuzar, Z.; Kratochvil, P. In Surface and Colloid Science; Matijevic, E., Ed.; Plenum: New York, 1993; Vol. 15.
7. Mountrichas, G.; Pispas, S. J Polym Sci Part A: Polym Chem 2007, 45, 5790–5799.
8. Alexandridis, P.; Lindman, B.; Amphiphilic Block Copolymers: Self-Assembly and Applications; Elsevier: Amsterdam, 2000.
9. Chen, J. T.; Thomas, E. L.; Ober, C. K.; Mao, G. P. Science 1996, 273, 343–346.
10. Jenekhe, S. A.; Chen, X. L. Science 1998, 279, 1903–1907.
11. Cornelissen, J. J.; Fischer, M.; Sommerdijk, N. A.; Nolte, R. J. M. Science 1998, 280, 1427–1430.
12. Stupp, S. I.; LeBonheur, V.; Walker, K.; Li, L. S.; Huggins, K. E.; Keser, M.; Amstutz, A. Science 1997, 276, 384–389.
13. Halperin, A. Macromolecules 1990, 23, 2724–2731.
14. Semenov, A. N. Mol Cryst Liq Cryst 1991, 209, 191–199.
15. Williams, D. R. M.; Fredrickson, G. H. Macromolecules 1992, 25, 3561–3568.
16. Matsen, M. W.; Barrett, C. J Chem Phys 1998, 109, 4108–4118.
17. Bellomo, E. G.; Wyrsta, M. D.; Pakstis, L.; Pochan, D. J.; Deming, T. J. Nat Mater 2004, 3, 244–248.
18. Ibarboure, E.; Rodriguez-Hernandez, J.; Papon, E. J Polym Sci Part A: Polym Chem 2006, 44, 4668–4679.
19. Abraham, S.; Ha, C. S.; Kim, I. J Polym Sci Part A: Polym Chem 2006, 44, 2774–2783.

20. Deng, C.; Chen, X.; Sun, J.; Lu, T.; Wang, W.; Jiang, X. J Polym Sci Part A: Polym Chem 2007, 45, 3218–3230.

21. Klok, H. A.; Langenwalter, J. F.; Lecommandoux, S. Macromolecules 2000, 33, 7819–7826.

22. Wu, J.; Pearce, E. M.; Kwei, T. K. Macromolecules 2002, 35, 1791–1796.

23. Sinaga, A.; Pavi, P.; Hatton, A.; Tam, K. C. J Polym Sci Part A: Polym Chem 2007, 45, 2646–2656.

24. Onouchi, H.; Hasegawa, T.; Kashiwagi, D.; Ishiguro, H.; Maeda, K.; Yashima, E. J Polym Sci Part A: Polym Chem 2006, 44, 5039–5048.

25. Block, H. Poly(*g*-benzyl-L-glutamate) and Other Glutamic Acid Containing Polymers; Gordon and Breach, New York, 1983.

26. Flory, P. J. Proc R Soc London Ser A 1956, 234, 73–89.

27. Doty, P.; Bradbury, J. H.; Holtzer, A. M. J Am Chem Soc 1956, 78, 947–954.

28. Wada, A. J Polym Sci 1960, 45, 145–154.

29. Powers, J. C.; Peticolas, W. L. Biopolymers 1970, 9, 195–203.

30. Kihara, H. Polym J 1977, 9, 443–450.

31. Sakamoto, R. Rep Prog Polym Phys Jpn 1980, 22, 699–702.

32. Ushiki, H.; Mita, I. Polym J 1984, 16, 751–759.

33. Tohyama, K.; Miller, W. G. Nature 1981, 289, 813–815.

34. Uematsu, I.; Uematsu, Y. Adv Polym Sci 1984, 59, 37–73.

35. Hill, A.; Donald, A. M. Polymer 1988, 29, 1426–1432.

36. Jackson, C. L.; Shaw, M. T. Polymer 1990, 31, 1070–1084.

37. Horton, J. C.; Donald, A. M. Polymer 1991, 32, 2418–2427.

38. Shukla, P. Polymer 1992, 33, 365–372.

39. Prystupa, D. A.; Donald, A. M. Macromolecules 1993, 26, 1947–1955.

40. Cohen, Y.; Dagan, A. Macromolecules 1995, 28, 7638–7644.

41. Tipton, D. L.; Russo, P. S. Macromolecules 1996, 29, 7402–7411.

42. Robinson, C.; Ward, J. C. Nature 1957, 180, 1183–1184.

43. Yu, S. M.; Conticello, V. P.; Zhang, G.; Kayser, C.; Fournier, M. J.; Mason, T. L.; Tirrell, D. A. Nature 1997, 389, 167–170.

44. Kim, K. T.; Park, C.; Vandermeulen, G. W. M.; Rider, D. A.; Kim, C.; Winnik, M. A.; Manners, I. Angew Chem Int Ed 2005, 44, 7964–7968.

45. Degee, P.; Dubois, P.; Jerome, R.; Teyssie, P. J Polym Sci Part A: Polym Chem 1993, 31, 275–278.

46. Cho, C. S.; Na, J. W.; Jeong, Y. I.; Kim, S. H.; Lee, Y. M.; Sung, Y. K. Polymer 1995, 19, 926–936.

47. Cheon, J. B.; Kim, B. C.; Park, Y. H.; Park, J. S.; Moon, J. Y.; Nahm, J. H.; Cho, C. S. Macromol Chem Phys 2001, 202, 395–400.

48. Zalipsky, S.; Hansen, C. B.; Oaks, J. M.; Allen, T. M. J Pharm Sci 1996, 85, 133–137.

49. Velander, W. H.; Madurawe, R. D.; Subramanian, A.; Kumar, G.; Sinai-Zingde, G.; Riffle, J. S. Biotechnol Bioeng 1992, 39, 1024–1030.

50. Woodle, M. C.; Engbers, C. M.; Zalipsky, S. Bioconjugate Chem 1994, 5, 493–496.

51. Kobayashi, S. Prog Polym Sci 1990, 15, 751–823.

52. Aoi, K.; Okada, M. Prog Polym Sci 1996, 21, 151–208.

53. Chiu, T. T.; Thill, B. P.; Fairchok, W. J.; Advances in Chemistry Series 213: Water Soluble Polymers; Washington: American Chemical Society, 1986.

54. Kim, C.; Lee, S. C.; Shin, J. H.; Yoon, J. S.; Kwon, I. C.; Jeong, S. Y. Macromolecules 2000, 33, 7448–7452.

55. Park, J.-S.; Akiyama, Y.; Winnik, F. M.; Kataoka, K. Macromolecules 2004, 37, 6786–6792.

56. Daly, W. H.; Poche, D. Tetrahedron Lett 1988, 29, 5859–5862.

57. Lee, S. C.; Chang, Y.; Yoon, J. S.; Kim, C.; Kwon, I. C.; Kim, Y. H.; Jeong, S. Y. Macromolecules 1999, 32, 1847–1852.

58. Yu, B.G.; Okano, T.; Kataoka, K.; Kwon, G. J Controlled Release 1998, 53, 131–136.

59. Hirst, A. R.; Smith, D. K.; Feiters, M. C.; Geurts, H. P. M.; Wright, A. C. J Am Chem Soc 2003, 125, 9010–9011.

60. Lecommandoux, S.; Achard, M. F.; Langenwalter, J. F.; Klok, H. A. Macromolecules 2001, 34, 9100–9111.

61. Antonietti, M.; Forster, S. Adv Mater 2003, 15, 1323–1333.

62. Raez, J.; Manners, I.; Winnik, M. A. J Am Chem Soc 2002, 124, 10381–10395.